Finite element modeling of acoustic emission in dry cask storage systems generated by cosine bell sources

Cite as: AIP Conference Proceedings **2102**, 130001 (2019); https://doi.org/10.1063/1.5099851
Published Online: 08 May 2019

Li Ai, Bruce Greer, Joseph Hill, et al.

Finite Element Modeling of Acoustic Emission in Dry Cask Storage Systems Generated by Cosine Bell Sources

Li Ai, Bruce Greer, Joseph Hill, Vafa Soltangharaei, Rafal Anay

Paul Ziehl[a]

University of South Carolina, Department of Civil and Environmental Engineering, Columbia, SC, USA

[a)] Corresponding author: ziehl@ce.sc.edu

Abstract. Dry cask storage system (DCSS) canisters used for the storage of high-level nuclear waste has begun to exceed the time for which they were originally intended. Therefore, efforts are being pursued by the nuclear industry to ensure that the structural integrity is maintained until arrangements have been made to transport the waste to a central repository. In this study, the technical basis of using acoustic emission monitoring for the detection of crack initiation and propagation in canister walls or welds in real time is investigated. The focus of this study, which is part of a larger project, is to develop the technical basis for using AE to monitor DCSS canisters for the initiation and propagation of stress corrosion cracking (SCC). SCC induced by a buildup of chlorides on the surface of the canister is postulated to be a potential degradation mechanism; however, there have been no known cases of this being found in practice. A small-scale type 304 stainless-steel specimen was utilized in this experiment to initiate and propagate stress corrosion cracking. Based on the experimental setup, a finite element model was built to investigate the feasibility of wave propagation modeling on small-scale type 304 stainless-steel specimens. Results indicate that wave propagation can be simulated by utilizing an excitation source. The model will later be applied to larger specimens that are similar in size to full-scale DCSS canisters.

INTRODUCTION

Nuclear power generation has been widely applied in the United States for decades. Currently, spent fuel is stored in cooling pools and dry cask storage systems (DCSS). DCSS use was initiated in the 1970s. Spent fuels are placed in stainless-steel canisters, then water and air are removed and replaced by inert gas. Many DCSS that were originally intended to contain waste products for 20 years are still in service (USNRC 2017). In some cases, these canisters are being inspected and re-licensed for another 40 years. One issue with extending the life of the containers is that stainless steel may be subject to degradation over time, such as stress corrosion cracking, crevice corrosion, and intergranular attack. Since DCSS are being re-licensed for another 40 years, the in-situ examination for detection of defects is desirable and challenging because canisters are stored in a concrete overpack that challenges the delivery of visual examination cameras and nondestructive examination sensors.

Acoustic emission (AE) is a nondestructive monitoring technique which is useful for detection of crack growth in many materials, sometimes utilizing pattern recognition approaches [1-4]. Amer et al. [5] investigated acoustic emission for identifying fatigue cracks in nuclear componentry made of 304H stainless-steel and found that acoustic emission signals could be classified into three different clusters. Babu et al. [6] utilized AE testing on blanket applications in fusion reactors to investigate the control of fatigue cracking. The blanket applications investigated were made of reduced activation ferritic-martensitic steel. This work reported a phenomenon similar with the results of Amer – namely that signals related to cracking and crack closure are discontinuous and can be classified in different clusters. Yu et al. [7] analyzed AE data from cruciform fillet welded joints in steel bridge material, finding that AE signals from regions of stable crack growth were greater than those from the typical noise threshold, with AE signals from regions of unstable crack growth having the highest intensity. Du et al. [8] investigated corrosion in 304 stainless-steel using slightly acidic sodium chloride (NaCl) solution during slow strain rate testing. The AE data was characterized according to different sources (pitting, cracking, and bubbling). They found that the solution used to

45th Annual Review of Progress in Quantitative Nondestructive Evaluation, Volume 38
AIP Conf. Proc. 2102, 130001-1–130001-8; https://doi.org/10.1063/1.5099851
Published by AIP Publishing. 978-0-7354-1832-5/$30.00

produce the corrosion defects (1.5 mol/L H2SO4 + 0.5 mol/L NaCl) in the 304NG stainless-steel reliably resulted in SCC in the specimens.

In this study, acoustic emission signal recognition and frequency characterization is explored through crack generation and propagation in 304 stainless steel. Stress corrosion cracking was induced by applying eccentric load, creating tensile stresses on the top surface of a Type 304 stainless steel plate, and exposing it to an acidic Potassium Tetrathionate solution. Finite element modeling was employed to simulate wave propagation in the steel plate. AE data was experimentally generated through pencil lead break sources on the stainless-steel plate and compared to simulations of resulting surface displacements in the FE model. Future work will investigate simulated crack propagation as an excitation source.

MATERIALS AND EXPERIMENTAL SETUP

The steel plates used in this study were made of 304H stainless-steel (H for high carbon). The higher carbon level makes the material more readily sensitized to grain boundary attack. The specimens had dimensions of 305 mm × 311 mm × 16 mm (12 in. × 12.25 in. ×0.625 in.). They were fabricated with two perpendicular tabs on each specimen. The tabs, which were 4 in. (102 mm) square, were welded to the bottom face. Each tab contained a hole located 3 inches (76 mm) from the bottom face of the plate. These holes allowed for a 0.75 in. (19 mm) diameter bolt and nut to be inserted into through the tabs. Once tightened, compressive forces forced the welded tabs toward one another. This action created bending within the plate, producing tension and compression faces on either side along the central axis between the welded tabs. The outside surface in tension is where cracking was initiated with the help of a small notch that created a stress concentration. Details of the specimen dimensions and sensor layout are shown in Figure 1. The experimental setup is shown in Figure 2.

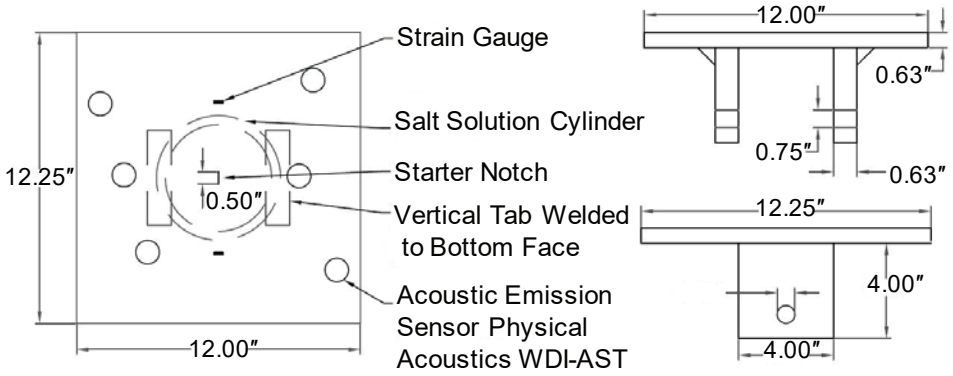

FIGURE 1. Specimen dimensions and sensor layout.

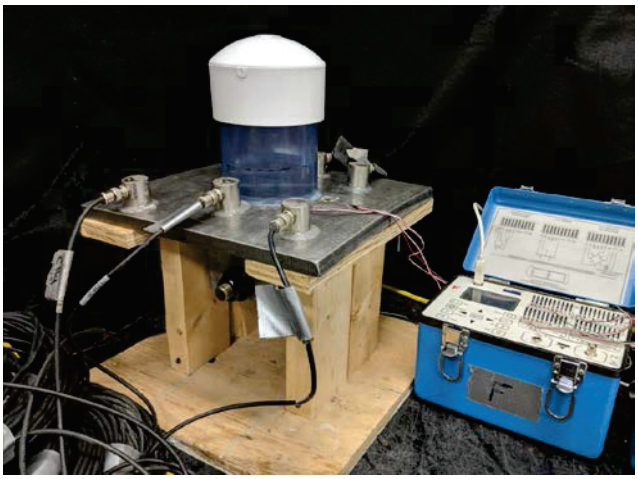

FIGURE 2. Experimental setup.

Prior to testing the target stress in the plates was calculated to ensure that yielding was avoided. Since 304H stainless steel has a yielding stress around 30,000 psi (206 MPa), the target stress was set at 27,000 psi (186 MPa). The target stress is based on theoretical values of weld residual stresses in the canister shell welds.

NUMERICAL MODEL

Finite element modeling was employed for the simulation of wave propagation [9-11]. The model in this study is a pencil lead break model, as this is a widely utilized and readily available source to represent acoustic emission signals [12-14]. The excitation source in the FE model is simulated by a cosine bell point source with characteristics shown below [15].

$$F(t) = 0\ N \qquad t < 0 \qquad (1)$$

$$F(t) = 0.5 - 0.5 \times \cos((\pi \times t)/T)N \qquad 0 < t < T \qquad (2)$$

$$F(t) = 1\ N \qquad t > T, T = 1\mu s \qquad (3)$$

Characteristics of the simulated source are shown graphically in Figure 3.

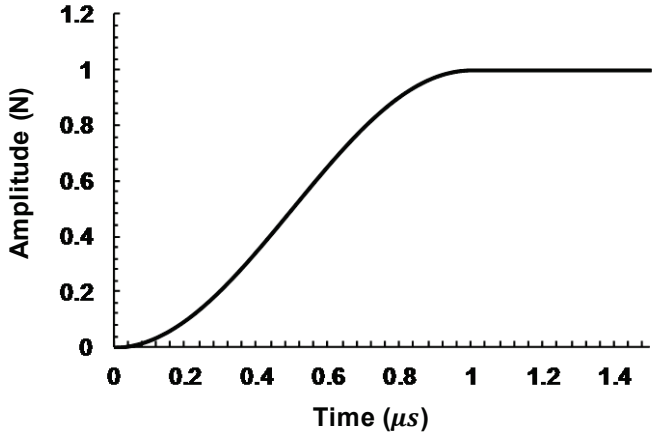

FIGURE 3. Cosine bell source, after [15].

The 3D FE model has the same dimensions as the experimental specimens, Figure 4. The simulated pencil lead break (cosine bell source) was input at the ends of the starter notch (shown as 'pencil lead break' in Figure 4). Observation points (for example, labeled as 'Point' in Figure 4) were included to capture the modeling results, which in this case are functions of surface displacement versus time. Comparative studies were undertaken to gain insight into the relationships between the wave propagation results in the FE model and the experimentally generated data (in this case a pencil lead break).

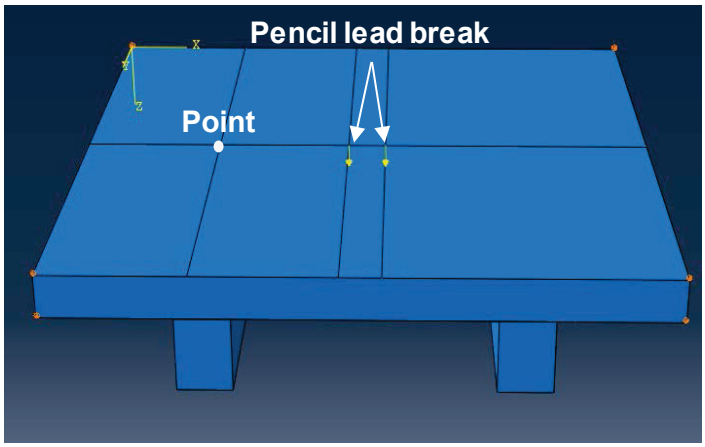

FIGURE 4. Finite element model representation.

A series of experimental pencil lead breaks (at least 5 breaks at each sensor) was conducted on the top surface of the specimen beside each of the six sensors. For illustration, the data described here refers to an experimental pencil lead break conducted next to sensor 1 (Figure 5). The simulated excitation sources in the finite element model were applied at the same location. While the transfer function of the sensors is not fully known, for this study the reasonable assumption is made that the sensors are primarily sensitive to out of plane displacement. Point 1 and Point 2 were setup in the FE model to capture resulting out of plane displacements for comparison of simulated to experimentally gathered results. Detailed geometry of the sensor layout and corresponding finite element model are shown in Figure 5.

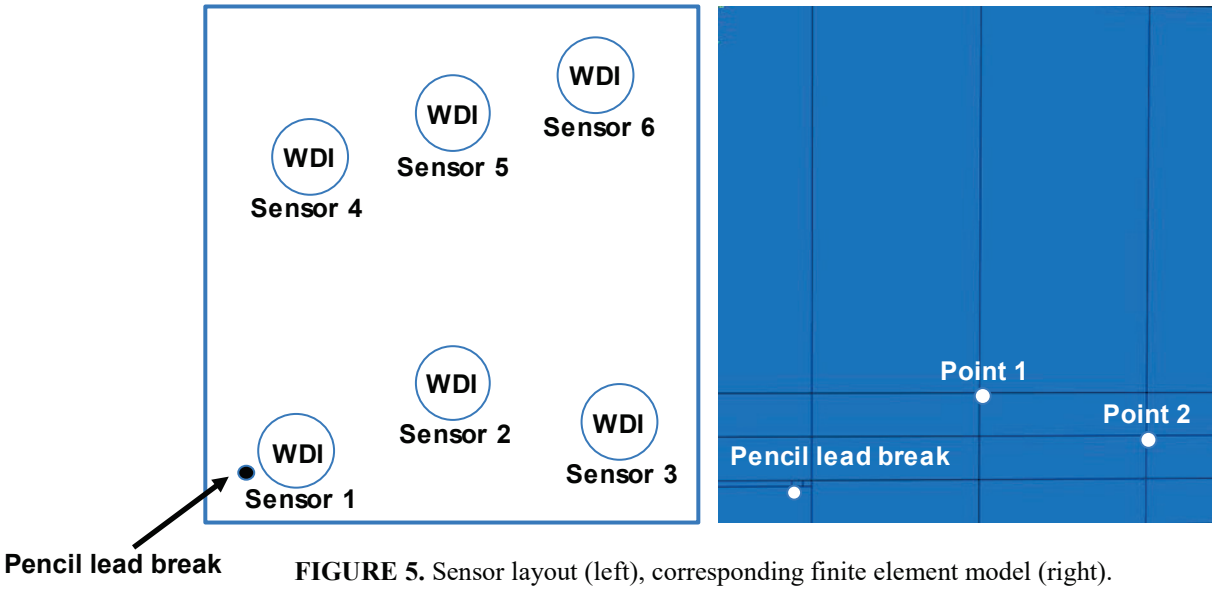

FIGURE 5. Sensor layout (left), corresponding finite element model (right).

RESULTS AND DISCUSSION

Figure 6 shows out of plane displacement results in different time steps where the wave is propagating from the notch tips. This figure represents the expected wave propagation, in terms of out of plane displacement, from the active crack extension due to stress corrosion cracking.

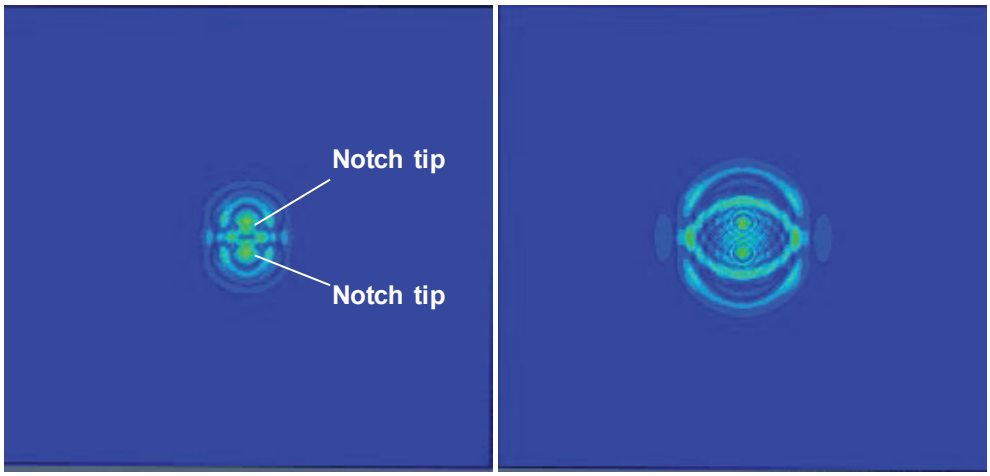

FIGURE 6. Wave propagation results.

The feasibility of utilizing FE modeling to inform decision making for different sensor types for optimized selection and placement is one focus of this study. Figure 7 compares the AE sensor response and FE model results (in terms of out of plane displacement) at observation point 2 (sensor 2). Figure 8 shows similar comparative results for observation point 3 (sensor 3). In Figures 7 and 8, the experimentally gathered and FE model results have been normalized in terms of amplitude. To compare results in the frequency domain, a Fast Fourier Transformation analysis was conducted, and results are presented below the results in the time domain in each figure. The magnitude of the finite element model results from 0 to 100 kHz is much larger in comparison to the experimentally gathered AE data.

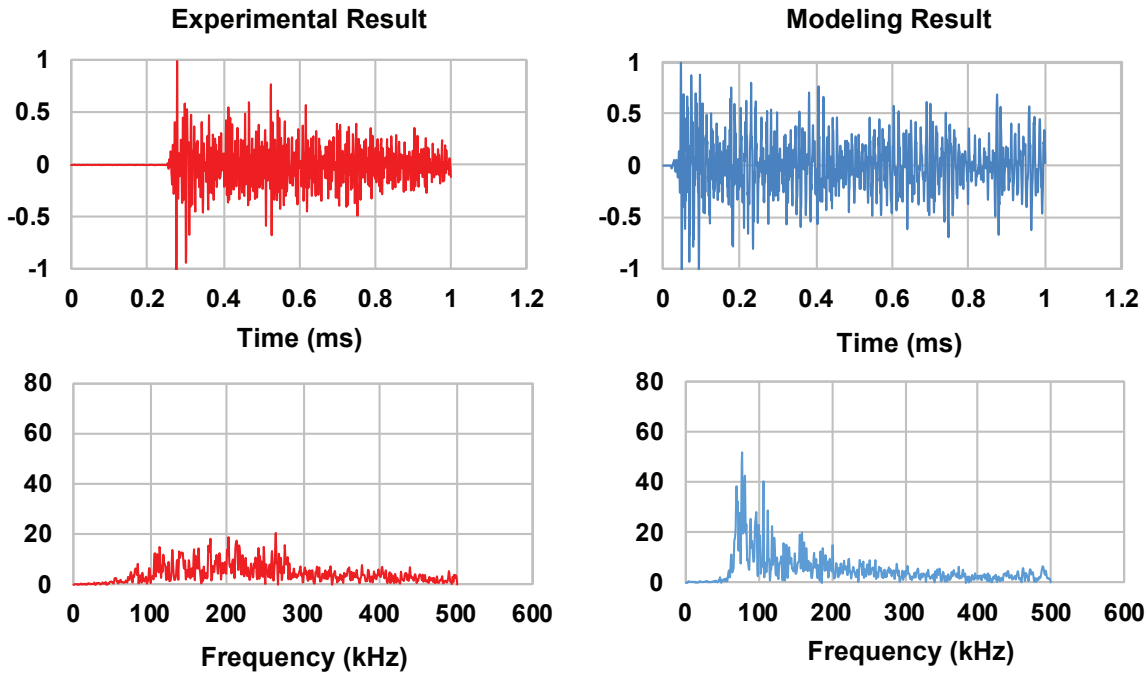

FIGURE 7. Experimental result (left), simulation result (right) - Sensor 2.

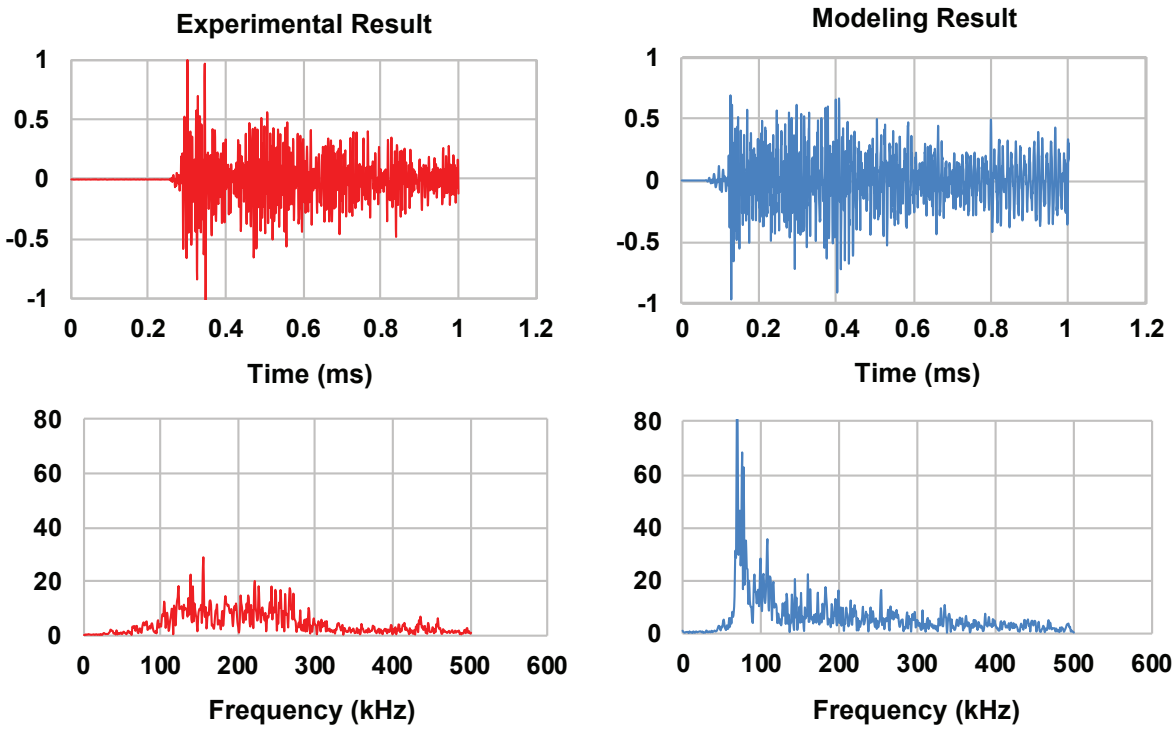

FIGURE 8. Experimental result (left), simulation result (right) - Sensor 3.

To investigate and better quantify the correlation between the experimental and simulated data, a correlation analysis was conducted (Figure 9). The correlation coefficient from 100 to 500 kHz is 0.40 for sensor 2 and 0.35 for sensor 3, both having a P-value < 0.001. The correlation coefficient from 0 to 100 kHz is 0.18 for sensor 2 and 0.13 for sensor 3, with P-value < 0.001 and P-value < 0.05. This analysis indicates that the correlation between the experimental data and the simulated data from 100 to 500 kHz is much higher than that from 0 to 100 kHz as expected due to the known sensor response in this frequency range. Furthermore, the correlation was influenced by the distance between source and sensor, with the larger distance having a lower correlation coefficient. This may be influenced by the value for damping used in the simulation.

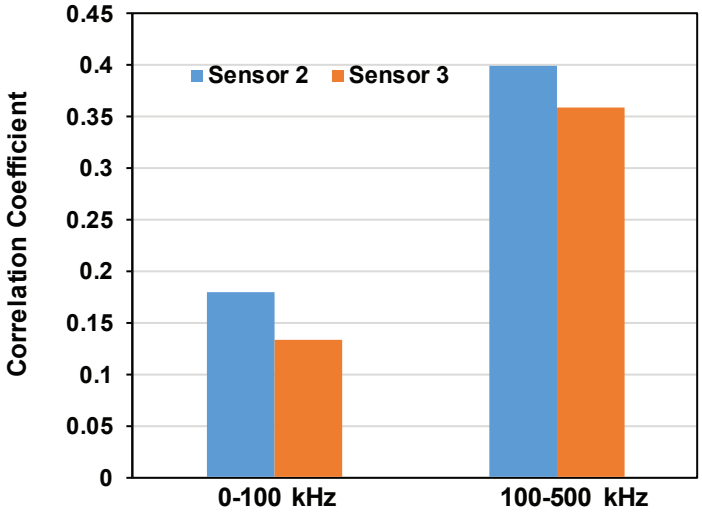

FIGURE 9. Correlation coefficient between experimentally gathered and simulated results - Sensors 2 and 3.

CONCLUSIONS & PERSPECTIVE

In this study, pencil lead breaks were conducted on stainless steel specimens having a starter notch placed into tension on the specimen surface. To compare experimentally gathered results to simulated results, acoustic emission sensors were utilized to record signals from the breaking of pencil leads on the specimen surface and this data was then compared to out of plane displacements simulated through finite element modeling.

Pertinent conclusions are:

1. Reasonable agreement was found between the simulated and experimentally gathered data in the known frequency response range of the sensors selected. This is encouraging as it indicates that simulation may be a useful approach for sensor selection and optimization of sensor placement.

2. As the distance from source to sensor was increased, the correlation between experiment and simulation decreased. Therefore, a compatible definition of damping may be required to guide further studies.

3. Future studies would benefit from the modeling of more realistic acoustic emission sources, such as those associated with crack extension, as well as a realistic model of the sensor itself.

Next steps for this study include incorporation of a compatible damping model and excitation sources like those associated with crack propagation. Geometrical spreading models [16] along with fracture mechanics relationships will be investigated [17].

ACKNOWLEDGMENTS

This research is based upon work partially supported by the Electrical Power Research Institute.

REFERENCES

[1] R. Liptai, D. Harris, C. Tatro, An introduction to acoustic emission, (ASTM STP 1972) **505**, p. 3–10.

[2] R. Anay, V. Soltangharaei, L. Assi, T. DeVol, P. Ziehl, "Identification of damage mechanisms in cement paste based on acoustic emission", *Construction and Building Materials* **164**, 286-296 (2018).

[3] L. Assi, V. Soltangharaei, R. Anay, P. Ziehl, F. Matta, "Unsupervised and supervised pattern recognition of acoustic emission signals during early hydration of Portland cement paste", *Cement and Concrete Research* **103**, 216-225 (2018).

[4] V. Soltangharaei, R. Anay, L. Assi, P. Ziehl, F. Matta, "Damage identification in cement paste amended with carbon nanotubes", in Proceedings, 44st Annual Review of Progress in Quantitative Nondestructive Evaluation, Utah, 2017, edited by D.E. Chimenti and L.J. Bond, (AIP, Conference Proceedings, # 1949, 2018), 030006.

[5] A.O. Amer, A.-L. Gloanec, S. Courtin, C. Touze, "Characterization of fatigue damage in 304L steel by an acoustic emission method", *Procedia Engineering* **66**, 651-660 (2013).

[6] M.N. Babu, C. Mukhopadhyay, G. Sasikala, S.K. Albert, A. Bhaduri, T. Jayakumar, R. Kumar, "Study of fatigue crack growth in RAFM steel using acoustic emission technique", *Journal of Constructional Steel Research* **126**, 107-116 (2016).

[7] J. Yu, P. Ziehl, F. Matta, A. Pollock, "Acoustic emission detection of fatigue damage in cruciform welded joints", *Journal of Constructional Steel Research* **86**, 85-91 (2013).

[8] G. Du, J. Li, W. Wang, C. Jiang, S. Song, "Detection and characterization of stress-corrosion cracking on 304 stainless steel by electrochemical noise and acoustic emission techniques", *Corrosion Science* **53**, 2918-2926 (2011).

[9] C. Willberg, J.M. Vivar-Perez, Z. Ahmad, U. Gabbert, Proceedings of The 7th International Workshop on Structural Health Monitoring, Simulation of piezoelectric induced Lamb wave motion in plates, edited by Fu-Kuo Chang, (Stanford, CA, 2009) pp. 2299-2307.

[10] B. Hosten, M. Castaings, "Finite elements methods for modeling the guided waves propagation in structures with weak interfaces", *Journal of the Acoustical Society of America* **117**, 1108-1113 (2005).

[11] M.V. Predoi, M. Castaings, L. Moreau, "Influence of material viscoelasticity on the scattering of guided waves by defects", *Journal of the Acoustical Society of America* **124**, 2883-2894 (2008).

[12] A. Nielsen, "Acoustic emission source based on pencil lead breaking", (The Danish Welding Institute Publication, 1980) **80**, p. 15.
[13] M.A. Hamstad, "Small diameter waveguide for wideband acoustic emission", *Journal of Acoustic Emission* **24**, 234-247 (2006).
[14] W. Prosser, M.A. Hamstad, J. Gary, A. OGallagher, "Reflections of AE waves in finite plates: finite element modeling and experimental measurements", *Journal of Acoustic Emission* **24**, 234-247 (1999).
[15] A.-M. Zelenyak, M.A. Hamstad, M.G. Sause, "Modeling of acoustic emission signal propagation in waveguides", *Sensors* **15**, 11805-11822 (2015).
[16] K. Ono, "Review on Structural Health Evaluation with Acoustic Emission", *Applied Sciences* **8**, 958 (2018).
[17] M.G. Sause, S. Richler, "Finite element modelling of cracks as acoustic emission sources", *Journal of Nondestructive Evaluation* **34**, 4 (2015).